【 CASE REPORT 】

An Autopsy Report of a Case with Cerebral Infarction Complicated by Coronavirus Disease 2019 Infection

Ryoji Goto[1,2], Haruka Kawakami[1], Yurino Horiuchi[1], Ayaka Chikada[1], Tsutomu Yasuda[1],
Tetsuya Suzuki[3], Yusuke Miyazato[3], Masahiro Ishikane[3], Yuya Kishino[4,5], Hideki Miyazaki[4],
Toru Igari[4], Harutaka Katano[6], Tadaki Suzuki[6], Shigeo Murayama[7,8] and Noritoshi Arai[1]

Abstract:

We herein report a case of cerebral infarct in a patient with coronavirus disease 2019 (COVID-19) infection who died of aspiration pneumonia. The postmortem examination of the brain revealed embolic infarct with negative findings on quantitative reverse transcription polymerase chain reaction (qRT-PCR) as well as immunohistochemistry to detect severe acute respiratory syndrome coronavirus 2 (SARS-CoV-2). The systemic examination only revealed low copy numbers of SARS-CoV-2 in the bronchus. This is the first and so far only autopsy case of COVID-19 infection with pathologic and virologic findings of the postmortem brain in Japan.

Key words: coronavirus disease 2019 (COVID-19), neuroinfectious disease, thrombus, infarction, stroke

Introduction

Coronavirus disease 2019 (COVID-19) has been associated with various neurological complications (1). However, its pathophysiology remains to be elucidated, and the importance of neuropathological study has been pointed out (2). Pathological autopsy is considered necessary for such a study, but autopsy studies of the brain have been limited.

We herein report a patient with COVID-19 for whom a brain autopsy was performed.

Case Report

The patient was an 80-year-old man who had been prescribed both aspirin and prasugrel due to recent percutaneous coronary intervention for unstable angina in addition to diabetes, hypertension, and dyslipidemia. He was not obese and had never been found to have any pulmonary diseases, nor did he smoke. He had never been vaccinated against severe acute respiratory syndrome coronavirus 2 (SARS-CoV-2), since this case occurred before the vaccination program had started in Japan.

He was found collapsed at home and was transported to our hospital, presenting with an impaired consciousness, body temperature of 37.6°C, and oxygen saturation on room air of 91%. The Glasgow Coma Scale (GCS) score was 12/15 (E3V3M6) then. A physical examination identified fine crackles bilaterally, while a neurological examination revealed left hemiplegia. Laboratory data showed severe inflammation with significant elevation of fibrinogen and D-dimer, while the values of prothrombin time (PT), activated partial thromboplastin time (APTT), and platelet count were normal. HbA1c was 7.6%, and low-density lipoprotein cho-
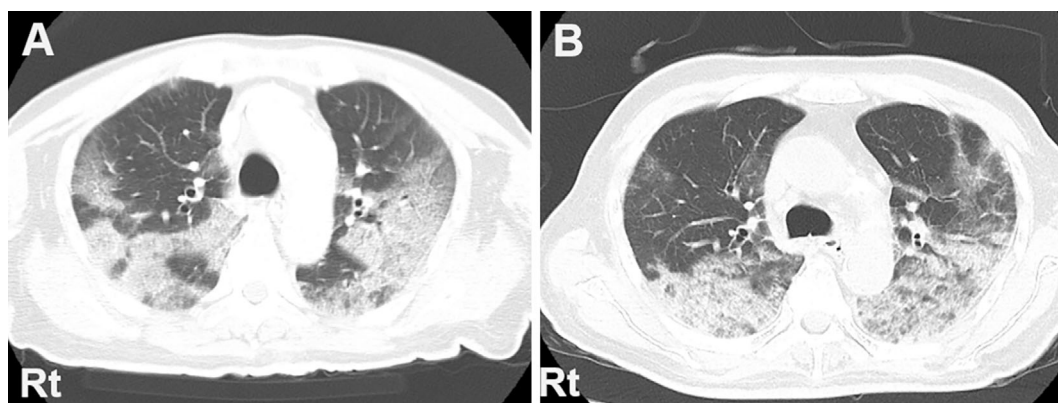
Figure 1. Chest computed tomography (CT) on admission reveals extensive sliver shadows in the bilateral lung fields in a map-like pattern (A). The shadows are mildly enhanced with consolidation in some areas on day 15, and some part of them shows signs of organizing pneumonia (B). Rt: right side

lesterol (LDL-C) was 98 mg/dL at the time of admission. Quantitative reverse transcription polymerase chain reaction (qRT-PCR) for SARS-CoV-2 at our hospital showed a positive result. Head computed tomography (CT) depicted cerebral infarction in the perfusion zone of the right middle cerebral artery. Chest CT revealed extensive consolidation in the lung fields bilaterally (Fig. 1).

We continued the 2 antiplatelet agents he was already taking and added heparin, starting at 10,000 units/day and tapering to 6,000 units/day because of prolonged APTT, along with remdesivir 100 mg/day, dexamethazone 6.6 mg/day, and ceftriaxone 2,000 mg/day. On day 2 of hospitalization, he developed non-ST-segment elevation myocardial infarction (NSTEMI) and was treated by nicorandil. His respiratory status gradually improved, and on day 11, we released him from isolation without performing additional qRT-PCR, according to the national COVID-19 management guideline in Japan (3). However, his GCS score had declined to 9/15 (E3V2M4), and his other neurological symptoms had not improved since admission. Head magnetic resonance imaging (MRI) on day 14 revealed widely distributed infarction (Fig. 2). However, on day 12, aspiration pneumonia caused his fever and breathing problems to reoccur (Fig. 1B). We started ceftriaxone and then switched it to sulbactam/ampicillin and teicoplanin, but he died on day 21 from respiratory failure. His vital signs had been monitored since admission, and we had not detected any signs of atrial fibrillation during the clinical course.

Autopsy was performed 16 hours after his death. In the lungs, alveolar pneumonia with neutrophilic infiltration into the alveoli was observed (Fig. 3A). It accompanied diffuse alveolar damage (DAD) in the exudative phase (Fig. 3B, C) as well as acute fibrinous and organizing pneumonia (AFOP) (Fig. 3D, E). Furthermore, irregular fibrosis with an older time phase was scattered (Fig. 3F), and fibrin thrombi were observed in a small number of pulmonary vessels (Fig. 3G). There were no findings of note in the bronchi (Fig. 3H). Myocardial infarct was identified, in addition to organized thrombus in the left ventricle. No thrombi were

detected in the atria, and we found no cardiac valvular vegetations, although the coronary arteries were highly atherosclerotic, with severe peripheral stenosis. Atherosclerosis was also severe in the abdominal aorta, whereas it was mild in the thoracic aorta.

The brain weight was 1,250 g before fixation. Although intravascular emboli were not observed and the atherosclerotic lesions of the cerebral arteries were mild, multiple subacute infarcts complicated by bleeding were found in the cerebral cortex (Fig. 4, 5A, B). Furthermore, microinfarcts were found in the pons, midbrain, and thalamus, accompanied by axonal swelling and edematous white matter (Fig. 5C, D). These were estimated to be newer than the infarcts of the cortex. We could not find any other pathological abnormalities, including in the olfactory tract and amygdala, nor any evidence of meningitis, encephalitis, or vasculitis, such as infiltration of inflammatory cells. Although the activation of microglial cells has been reported (4, 5), immunochemistry of CD68 for microglia and AT-8 for neurofibrillary tangles only revealed the accumulation of activated microglia around neuritic plaques.

We additionally investigated the presence of SARS-CoV-2 in the specimens, including the infarctions. Copy numbers of SARS-CoV-2 ribonucleic acid (RNA) were determined by qRT-PCR, using forward (5'-GGCCGCAAATTGCACAAT-3') and reverse (5'-CCAATGCGCGACATTCC-3') primers and a labeled probe 5'-(FAM)-CCCCCAGCGCTTCAGCGTTCT-(TAMRA)-3' (6). However, SARS-CoV-2 RNA was detected only in the sample from the bronchi, and even then only at a low copy number (523 copies per 100 ng of total RNA) by qRT-PCR. Furthermore, immunohistochemistry for SARS-CoV-2 was performed by the polymer-immunocomplex method using an EnVision System (Dako, Carpinteria, USA) with primary antibodies against the SARS-CoV nucleocapsid protein (rabbit polyclonal; National Institute of Infectious Diseases, Tokyo, Japan), for which reactivity against SARS-CoV-2 has been confirmed (6); however, the SARS-CoV-2 antigen was not detected in any of the samples investigated (Table, Fig. 6).
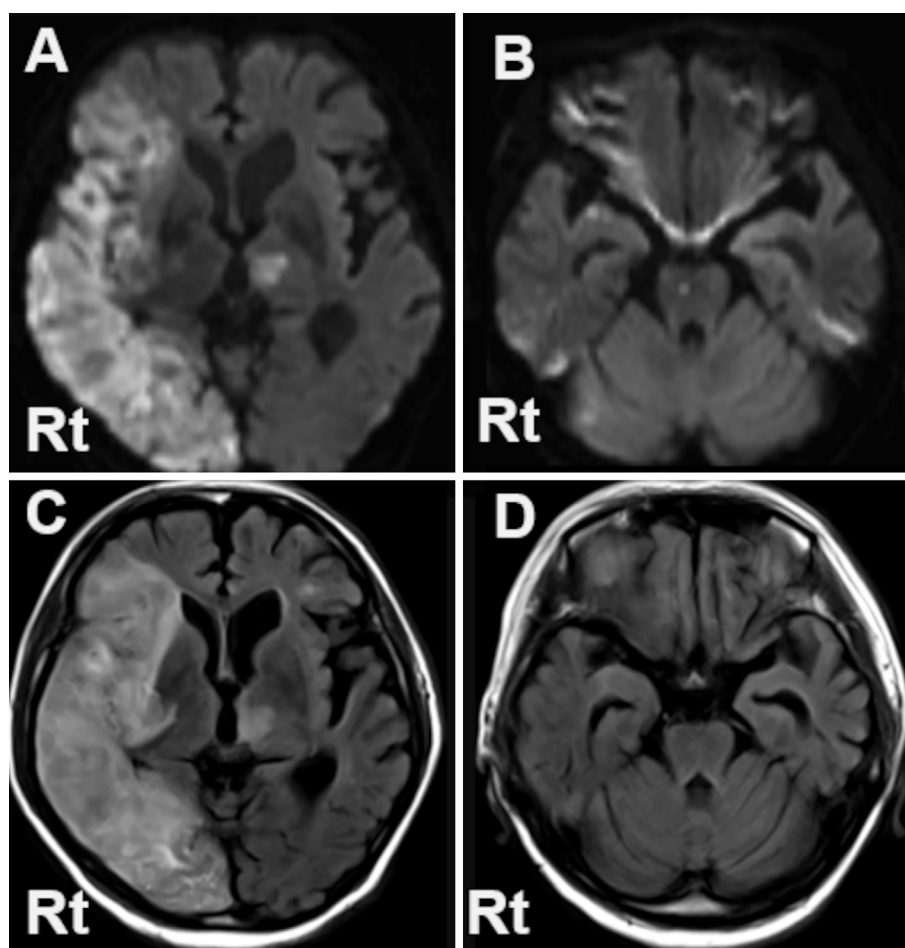
Figure 2. Diffusion weighted image (DWI) (A, B), and fluid-attenuated inversion recovery (FLAIR) image (C, D) of brain MRI taken on day 14. Marked hyperintensity on both DWI and FLAIR is observed extensively in the perfusion zone of the right middle cerebral artery and the right medial occipital artery, and also spottedly in the left thalamus (A, B). The abnormal signals are also seen in the pons and the bilateral cerebella on DWI (C), while they are not apparent on FLAIR (D). Rt: right side

Discussion

Regarding the pulmonary findings that caused the patient's death, DAD and AFOP were noted in the acute phase and therefore indicated to have been caused by aspiration pneumonia rather than COVID-19, considering the clinical course. In contrast, only the irregular fibrosis was considered to have been derived from COVID-19 pneumonia. SARS-CoV-2 was hardly detected by qRT-PCR or immuno-histochemistry, and even in the bronchi, where it was only detected, no significant findings were noted.

We detected both macroscopic infarcts and microinfarcts in the brain. In previous autopsy reports of COVID-19 patients, cerebral infarcts have been commonly described and were presumed to have been of thromboembolic origin because of their vascular pattern (7), although intravascular microthrombi had been less commonly reported (8). Despite the absence of intravascular emboli or clinical evidence of atrial fibrillation, the organized thrombus in the ventricle indicated the macroscopic infarcts to be cardioembolic; since

they were in the subacute phase, they may have occurred coincidentally with the onset of COVID-19, although we were unable to determine the relevance of infection at autopsy. In contrast, the microinfarcts appeared to have developed by a different etiology, considering their suspected newer onset and the blood flow distribution. The pathological findings, including the thrombi in pulmonary vessels, suggest that the microinfarcts were caused by microscopic vascular changes, similar to disseminated intravascular coagulation.

Taking into account the negative qRT-PCR and immuno-histochemistry results, the absence of those findings raises the possibility that the virus did not invade the brain parenchyma. However, the infarction may still have been associated with SARS-CoV-2, as it has been reported that viral RNA levels detected by qRT-PCR are very low and viral protein is not detected at all by immunohistochemistry in brains from some COVID-19 patients, all of whom were complicated with hypoxic/ischemic changes (9). It has been hypothesized that SARS-CoV-2 invasion into endothelial cells of brain vasculature via angiotensin-converting enzyme
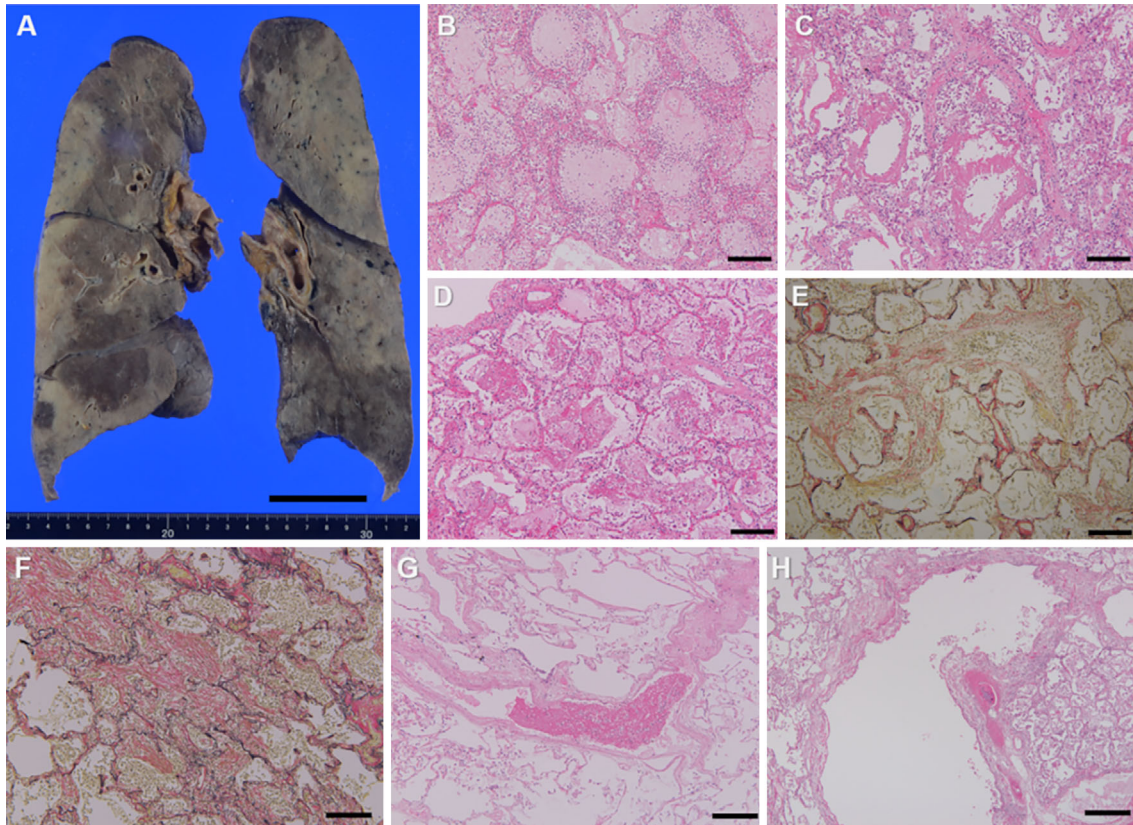
Figure 3. Coronal section of the lungs (A). Alveolar pneumonia with numerous neutrophilic infiltrates is seen mainly in the lower lobes of bilateral lungs (B). It extensively accompanies epithelial denudation and development of hyaline membranes with little collagen fiber (C), which indicates the exudative phase of diffuse alveolar damage. Fibrin balls are also seen in the alveolar spaces (D), and scattered loose fibrosis penetrating into the alveoli and alveolar canals are observed (E), which demonstrate acute fibrinous and organizing pneumonia. On the other hand, irregular fibrosis with older time phase are scattered (F), suggesting to be the scarring from coronavirus disease 2019 (COVID-19) pneumonia. Fibrin thrombi are observed in a small number of pulmonary vessels (G). There are no findings of note in the left bronchus (H). Hematoxylin and Eosin staining (B-D, G, H), Elastica van Gieson (EVG) stain (E, F). Scale bars: 5 cm (A), 100μm (B-G), 250 μm (H).
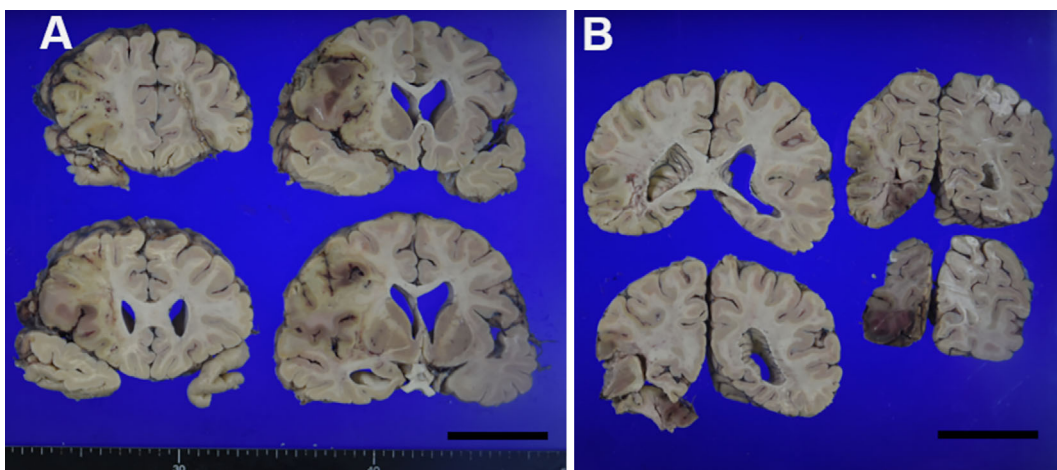

Figure 4. Coronal slices of the cerebrum show multiple infarctions with bleeding, mainly in the perfusion zone of the right middle cerebral artery. Scale bars: 5 cm (A, B)

2 (ACE2) receptor leads to microthrombi deposition (10). Furthermore, it can induce a systemic inflammatory response and a hypercoagulable state through the coagulation cascade and elevation of von Willebrand factor (vWF) (5, 10).
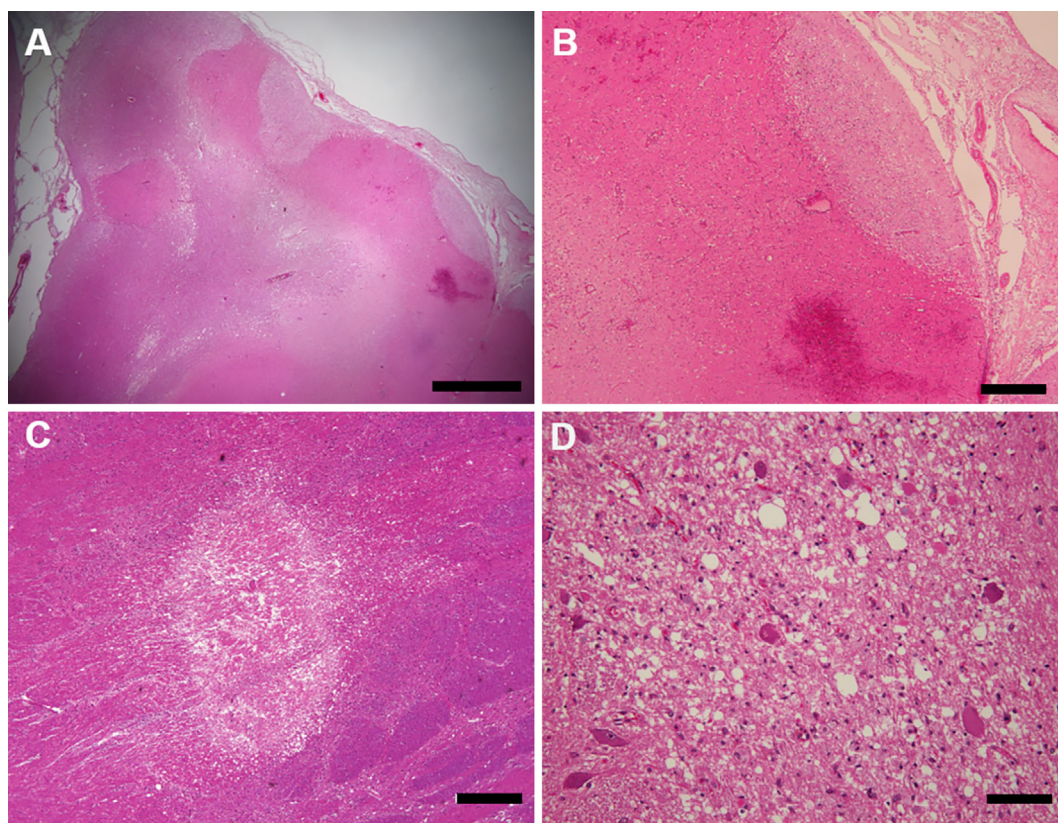
Figure 5. The lesion of subacute infarction complicated with hemorrhage is observed in the cortex of the postcentral gyrus (A). It is rarefacted and accompanies angiogenesis (B). The microinfarction observed in the midbrain (C) is accompanied by axonal swelling and edematous white matter (D). Hematoxylin and Eosin staining. Scale bars: 2 mm (A), 500 μm (B, C), 100μm (D)
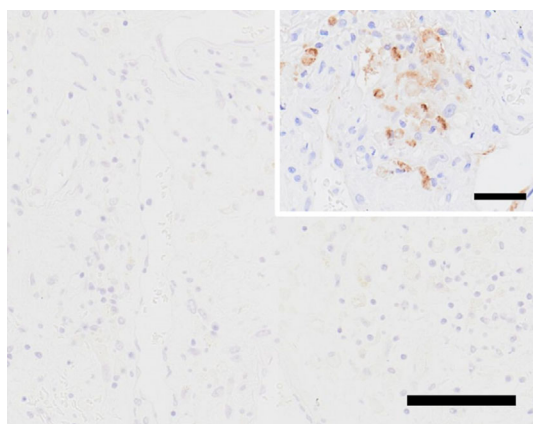

Figure 6. The infarct of the right frontal lobe showed negative on severe acute respiratory syndrome coronavirus 2 (SARS-CoV-2) immunohistochemistry. Inset: a positive control of SARS-CoV-2 immunohistochemistry in the lung of another unrelated patient. Alveolar epithelial cells are positive for SARS-CoV-2. Scale bars: 100μm, 50μm (inset)

Therefore, the infarction in our case may have been induced by the direct endotheliopathy and the indirect hypercoagulopathy caused by SARS-CoV-2.

It should be noted that autopsy in this case was performed in accordance with the normal infection control measures in autopsies using an anti-infection dissection room, as the patient had been released from isolation for COVID-19. A previous report showed that SARS-CoV-2 was more frequently detected in the bronchus than in the lung by qRT-PCR in autopsy cases (11), and another study demonstrated that no virus was detected in lung samples from the organizing phase of DAD after more than two weeks from the onset (12). In the present case, SARS-CoV-2 was detected only at the bronchus with low copy numbers by qRT-PCR and was undetectable in immunohistochemistry. This implies the presence of a low number of infectious viruses in the bronchus, suggesting their reduced infectivity compared with the acute phase of COVID-19.

In conclusion, we described autopsy of a brain from a COVID-19 patient complicated with cerebral infarction. While the autopsy results failed to provide evidence of the invasion of SARS-CoV-2 into the brain parenchyma, macroscopic embolism and microinfarctions were observed, with evidently different etiologies. Since SARS-CoV-2 may induce thrombosis by both endotheliopathy and hypercoagulopathy, the infection may have contributed to the development of the stroke. In elderly patients with risk factors, anticoagulation therapy should be introduced at the early stage of the disease because of the risk of developing severe stroke, as shown in this case. In addition, the low copy numbers of SARS-CoV-2 on qRT-PCR suggest a reduced infectivity at autopsy, so the further accumulation of autopsy

Table. Quantification of Severe Acute Respiratory Syndrome Coronavirus 2 (SARS-CoV-2) Ribonucleic Acid (RNA) and Immunohistochemistry against SARS-CoV-2 RNA in Multiple Specimens.

Specimen type/site	SARS-CoV-2, copies/reaction	SARS-CoV-2 immuno-histochemistry
Nasal swab	UDL	-
Right frontal lobe (with infarction)	UDL	Negative
Left frontal lobe (without infarction)	UDL	Negative
Left bronchus	523	Negative
Left lung		
Upper lobe (with AFOP)	UDL	Negative
Lower lobe (with AFOP)	UDL	Negative
Lower lobe (without AFOP)	UDL	Negative
Right bronchus	UDL	Negative
Right lung		
Upper lobe (with AFOP)	UDL	Negative
Upper lobe (without AFOP)	UDL	Negative
Middle lobe (without AFOP)	UDL	Negative
Lower lobe (with AFOP)	UDL	Negative
Left ventricle of the heart	UDL	Negative
Liver		
Left lobe	UDL	Negative
Right lobe	UDL	Negative
Spleen	UDL	Negative
Left adrenal gland	UDL	Negative
Left kidney	UDL	Negative

UDL: under detection limit (<10 copies/reaction), AFOP: acute fibrinous and organizing pneumonia

findings, including those involving the brain, is required to elucidate the pathogenesis of COVID-19.

The authors state that they have no Conflict of Interest (COI).

References

1. Ahmed MU, Hanif M, Ali MJ, et al. Neurological manifestations of COVID-19 (SARS-CoV-2): a review. Front Neurol **11**: 518, 2020.
2. Takao M. Important and unresolved aspects of neuropathologic analyses of COVID-19 individuals. Brain Nerve **72**: 1061-1065, 2020 (in Japanese with English abstract).
3. Ministry of Health, Labour and Welfare in Japan. National COVID-19 management guideline in Japan [Internet]. 2021 [cited 2021 Jan 29]. Available from: https://www.mhlw.go.jp/content/000 785119.pdf (in Japanese)
4. Al-Sarraj S, Troakes C, Hanley B, et al. Invited review: the spectrum of neuropathology in COVID-19. Neuropathol Appl Neurobiol **47**: 3-16, 2021.
5. Fisicaro F, Di Napoli M, Liberto A, et al. Neurological sequelae in patients with COVID-19: a histopathological perspective. Int J Environ Res Public Health **18**: 1-16, 2021.
6. Adachi T, Chong J, Nakajima N, et al. Clinicopathologic and immunohistochemical findings from autopsy of patient with COVID-19, Japan. Emerg Infect Dis **26**: 2157-2161, 2020.
7. Matschke J, Lütgehetmann M, Hagel C, et al. Neuropathology of patients with COVID-19 in Germany: a post-mortem case series. Lancet Neurol **19**: 919-929, 2020.
8. Mukerji SS, Solomon IH. What can we learn from brain autopsies in COVID-19? Neurosci Lett **742**: 135528, 2021.
9. Thakur KT, Miller EH, Glendinning MD, et al. COVID-19 neuropathology at Columbia University Irving Medical Center/New York Presbyterian Hospital. Brain **15**: awab148, 2021.
10. Boldrini M, Canoll PD, Klein RS. How COVID-19 affects the brain. JAMA Psychiatry **78**: 682-683, 2021.
11. Peiris S, Mesa H, Aysola A, et al. Pathological findings in organs and tissues of patients with COVID-19: a systematic review. PLoS One **16**: e0250708, 2021.
12. Schaefer IM, Padera RF, Solomon IH, et al. *In situ* detection of SARS-CoV-2 in lungs and airways of patients with COVID-19. Mod Pathol **33**: 2104-2114, 2020.